J.Natn.Sci.Foundation Sri Lanka 2013 41 (3): 209-217
DOI: http://dx.doi.org/10.4038/jnsfsr.v41i3.6053

RESEARCH ARTICLE

Inelastic electron scattering from light nuclei

F.I. Sharrad [1,2*], A.K. Hamoudi [3], R.A. Radhi [3] and H.Y. Abdullah [4,5]
[1] *Department of Physics, Faculty of Science, University of Malaya, Kuala Lumpur, Malaysia.*
[2] *Department of Physics, College of Science, University of Karbala, Karbala, Iraq.*
[3] *Department of Physics, College of Science, University of Baghdad, Baghdad, Iraq.*
[4] *Department of Physics, Universiti Teknologi Malaysia, Johor, Malaysia.*
[5] *Department of Physics, College of Science Education, Salahaddin University, Erbil, Iraq.*

Revised: 06 March 2013; Accepted: 19 April 2013

Abstract: The inelastic longitudinal form factors *F(q)*'s, an expression for the transition charge density were studied where the deformation in nuclear collective modes besides the shell model transition density are taken into consideration. In this work, the core polarization transition density was evaluated by adopting the shape of Tassie model together with the form of the ground state two-body charge density distributions and the effect of two body short range correlation function. It was noticed that the core polarization effects, which represent the collective modes are essential in obtaining a good agreement between the calculated inelastic longitudinal *F(q)*'s and those of the experimental data for ^{4}He, ^{12}C, ^{16}O, ^{28}Si, ^{32}S and ^{40}Ca nuclei.

Keywords: Core polarization, electron scattering, light nuclei, short range.

INTRODUCTION

Inelastic scattering of medium energy electrons provides a well-understood probe of the charge, current and magnetization densities, which characterize nuclear excitations (Millener *et al.*, 1989).

Hotta *et al.* (1988) measured inelastic electron scattering cross section for ^{4}He at 180º for incident electron energies of 130 and 200 MeV. Spectra measured up to excitation energies of 54 MeV, were relatively featureless and they showed no evidence of resolvable excitations. The longitudinal and transverse form factors for ^{12}C were determined separately as functions of the excitation energy from 15 − 40 MeV in the momentum transfer range 0.75 − 1.56 fm^{-1} (Yamaguchi *et al.*, 1971). The nuclear response to 200 − 350 MeV electrons inelastically scattered at 20º for six nuclei ranging from A = 9 to 181 was given. An excitation energy integral was formed and compared with theoretical calculations of the total inelastic scattering cross section (O'Connell *et al*., 1983). Inelastic electron scattering with high energy resolution was used by Miska *et al*. (1975) to study the states at 6.05 (0^{+}), 6.13 (3^{-}) and 6.92 (2^{+}) MeV excitation energy in ^{16}O for momentum transfers q = 0.22 – 0.49 fm^{-1}. Coulomb form factors of C4 transitions in even-even N = Z sd-shell nuclei (^{20}Ne, ^{24}Mg, ^{28}Si and ^{32}S) have been discussed previously (Radhi, 2003) taking into account the higher-energy configurations outside the sd-shell model space, which are called core polarization effects. Also inelastic electron scattering to 2^{+} and 4^{+} states for the even-even N = Z sd-shell nuclei have been discussed by Radhi & Boucheback (2003) considering the core-polarization effects. These effects were included through a microscopic theory that contains excitation from the core 1s and 1p orbits and also from 2s-1d shell to the higher allowed orbits with $2\hbar\omega$ excitation. These effects were found essential in both the transition strength and momentum transfer dependence of form factors and they gave remarkably good agreement with the data.

The purpose of the present work was to calculate the longitudinal C0, C2 and C4 form factors for the inelastic electron scattering ^{4}He, ^{12}C, ^{16}O, ^{28}Si, ^{32}S and ^{40}Ca nuclei depending on the ground state two-body charge density distributions, which included the effect of two-body short range correlation.

* Corresponding author (fadhil.altaie@gmail.com)

Inelastic longitudinal form factors

Inelastic longitudinal electron scattering form factors involve angular momentum J and momentum transfer q, which can be written as (Brown *et al*., 1985);

$$\left|F_J^L(q)\right|^2 = \frac{4\pi}{Z^2(2J_i+1)}\left|\left\langle f \left\| \hat{T}_J^L(q) \right\| i \right\rangle\right|^2 |F_{cm}(q)|^2 \, |F_{fs}(q)|^2 \quad ...(1)$$

where $\hat{T}_J^L(q)$ is the longitudinal electron scattering operator, $F_{fs}(q)$ is the finite nucleon size correction, $F_{cm}(q)$ is the center of mass correction and Z is the atomic number. The nuclear states have well defined isospin $T_{i/f}$ and therefore the form factors of equation 1 can be written in terms of the matrix elements reduced in both angular momentum and isospin (Donnelly & Sick, 1984).

$$\left|F_J^L(q)\right|^2 = \frac{4\pi}{Z^2(2J_i+1)}\left|\sum_{T=0,1}(-1)^{T_f-T_{z_f}}\begin{pmatrix} T_f & T & T_i \\ -T_{Z_f} & 0 & T_{Z_i}\end{pmatrix}\left\langle f \left\| \hat{T}_{JT}^L(q) \right\| i \right\rangle\right|^2 |F_{cm}(q)|^2 \, |F_{fs}(q)|^2 \quad ...(2)$$

where T is restricted by the following selection rule:

$$\left|T_f - T_i\right| \le T \le T_f + T_i \quad ...(3)$$

and $T_Z = \frac{Z-N}{2}$. The bracket ( ) in equation 2 is the three – J symbol, and the reduced matrix elements in spin and isospin space of the longitudinal operator between the final and initial many particles states of the system including configuration mixing are given in terms of the one-body density matrix (OBDM) elements times the single particle matrix elements of the longitudinal operator (Brussard & Glaudemans, 1977).

$$\left\langle f \left\| \hat{T}_{JT}^L \right\| i \right\rangle = \sum_{a,b} OBDM^{JT}(i,f,J,a,b)\left\langle b \left\| \hat{T}_{JT}^L \right\| a \right\rangle \quad ...(4)$$

The OBDM elements are calculated in terms of the isospin–reduced matrix elements (Brown *et al.*, 1983), i.e.

$$OBDM(\tau_Z) = (-1)^{T_f - T_z}\begin{pmatrix} T_f & 0 & T_i \\ -T_Z & 0 & T_Z\end{pmatrix}\sqrt{2}\ \frac{OBDM(\Delta T = 0)}{2} + \tau_Z(-1)^{T_f - T_z}\begin{pmatrix} T_f & 1 & T_i \\ -T_Z & 0 & T_Z\end{pmatrix}\sqrt{6}\,\frac{OBDM(\Delta T = 1)}{2} \quad ...(5)$$

The OBDM (ΔT) is defined (Brown *et al.*, 1983) as

$$OBDM(i,f,j,j',\Delta T) = \frac{\left\langle f \left\| \left[a_j^+ \times \tilde{a}_{j'}\right]^{J,\Delta T} \right\| i \right\rangle}{\sqrt{2J+1}\ \sqrt{2\Delta T+1}} \quad ...(6)$$

The operator a_j^+ creates a neutron or proton in the single nucleon state and the operator $\tilde{a}_{j'}$ annihilates a neutron or proton in the single nucleon state j'.

Core – polarization effects

The model space matrix elements are not adequate to describe the absolute strength of the observed gamma-ray transition probabilities, because of the polarization in nature of the core protons by the model space protons and neutrons (Radhi *et al*., 2002). Therefore many particle reduced matrix elements of the longitudinal operator consists of two parts; one is for the model space and the other is for the core polarization matrix element (Radhi & Aouda, 1997).

$$\left\langle f \left\| \hat{T}_J^L(\tau_Z,q) \right\| i \right\rangle = \left\langle f \left\| \hat{T}_J^{L\,ms}(\tau_Z,q) \right\| i \right\rangle + \left\langle f \left\| \hat{T}_J^{L\,core}(\tau_Z,q) \right\| i \right\rangle \quad ...(7)$$

where the model space matrix element in equation 7 has the form (Radhi & Aouda, 1997).

$$\left\langle f \left\| \hat{T}_J^{L\,ms}(\tau_Z,q) \right\| i \right\rangle = e_i \int_0^\infty d\mathrm{r}\, \mathrm{r}^2 j_J(q\mathrm{r})\, \rho^{ms}_{J,\tau_Z}(i,f,\mathrm{r}) \quad ...(8)$$

The model space transition density $\rho^{ms}_{J,\tau_Z}(i,f,\mathrm{r})$ is expressed as the sum of the product of the OBDM times the single particle matrix elements, and is given by (Brown *et al.*, 1983).

$$\rho^{ms}_{J,\tau_Z}(i,f,\mathrm{r}) = \sum_{jj'(ms)}^{ms} OBDM(i,f,J,j,j',\tau_z)\left\langle j \left\| \mathrm{Y}_J \right\| j' \right\rangle R_{nl}(\mathrm{r})\, R_{n'l'}(\mathrm{r}) \quad ...(9)$$

where $R_{nl}(\mathrm{r})$ is the radial part of the harmonic oscillator wave function.

The core- polarization matrix element in equation 7 takes the following form (Radhi & Aouda, 1997).

$$\left\langle f \left\| \hat{T}_J^{L\,core}(\tau_Z,q) \right\| i \right\rangle = e_i \int_0^\infty d\mathrm{r}\, \mathrm{r}^2 j_J(q\mathrm{r})\, \rho_J^{core}(i,f,\mathrm{r}) \quad ...(10)$$

where ρ_J^{core} is the core- polarization transition density,

which depends on the model used for core polarization. To take the core- polarization effects into consideration, the model space transition density is added to the core-polarization transition density that describes the collective modes of nuclei. The total transition density becomes,

$$\rho_{J\tau_Z}(i,f,\mathrm{r}) = \overset{ms}{\rho}_{J\tau_Z}(i,f,\mathrm{r}) + \overset{core}{\rho}_{J\tau_Z}(i,f,\mathrm{r}) \qquad ...(11)$$

According to the collective modes of nuclei, the core polarization transition density is given by the Tassie shape (Flaiyh, 2010),

$$\rho^{core}_{Jt_z}(i,f,\mathrm{r}) = N\frac{1}{2}(1+\tau_z)\,\mathrm{r}^{J-1}\frac{d\rho_o(i,f,\mathrm{r})}{d\mathrm{r}} \qquad ...(12)$$

where N is a proportionality constant and ρ_o is the ground state two – body charge density distribution, which is given as

$$\rho_o = \langle \Psi \mid \hat{\rho}^{(2)}_{eff}(\vec{\mathrm{r}}) \mid \Psi \rangle = \sum_{i<j}\langle i\ j \mid \hat{\rho}^{(2)}_{eff}(\vec{\mathrm{r}})\ [\mid ij\rangle - \mid ji\rangle\ ] \qquad ...(13)$$

where (Sharrad, 2007)

$$\hat{\rho}^{(2)}_{eff}(\vec{\mathrm{r}}) = \frac{1}{2(A-1)}\ f(r_{ij})\sum_{\mathrm{i}\neq\mathrm{j}}\left\{\delta(\vec{\mathrm{r}}-\vec{\mathrm{r}}_{\mathrm{i}}) + \delta(\vec{\mathrm{r}}-\vec{\mathrm{r}}_{\mathrm{j}})\right\} f(r_{ij}) \qquad ...(14)$$

also, i and j are all the required quantum numbers, i.e.

$$i \equiv n_i, l_i, j_i, m_i, t_i, m_{t_i} \quad \text{and} \quad j \equiv n_j, l_j, j_j, m_j, t_j, m_{t_j}$$

The functions $f(\mathrm{r_{ij}})$ are the two–body short range correlation (SRC). In this work, a simple model form of short range correlation by Sharrad (2007) will be adopted $f(\mathrm{r_{ij}}) = 1 - \exp[-\beta(\mathrm{r_{ij}} - \mathrm{r_c})^2]$ where $\mathrm{r_c}$ is the radius of a suitable hard–core and β is a correlation parameter.

The Coulomb form factor for this model becomes,

$$F^L_J(q) = \sqrt{\frac{4\pi}{2J_i+1}}\frac{1}{Z}\left\{\int_0^\infty \mathrm{r}^2 j_J(q\mathrm{r})\rho^{ms}_J(i,f,\mathrm{r})\,d\mathrm{r} + N\int_0^\infty d\mathrm{r}\,\mathrm{r}^2 j_J(q\mathrm{r})\mathrm{r}^{J-1}\frac{d\rho_o(i,f,\mathrm{r})}{d\mathrm{r}}\right\} F_{cm}(q)\,F_{fs}(q) \qquad ...(15)$$

The radial integral $\int_0^\infty d\mathrm{r}\ \mathrm{r}^{J+1} j_J(q\mathrm{r})\frac{d\rho_o(i,f,\mathrm{r})}{d\mathrm{r}}$ can be written as

$$\int_0^\infty \frac{d}{d\mathrm{r}}\left\{\mathrm{r}^{J+1} j_J(q\mathrm{r})\rho_o(i,f,\mathrm{r})\right\}d\mathrm{r} - \int_0^\infty d\mathrm{r}\ (J+1)\mathrm{r}^J j_J(q\mathrm{r})\rho_o(i,f,\mathrm{r}) - \int_0^\infty d\mathrm{r}\ \mathrm{r}^{J+1}\frac{d}{d\mathrm{r}} j_J(q\mathrm{r})\rho_o(i,f,\mathrm{r}) \qquad ...(16)$$

the first term gives zero contribution, the second and the third term can be combined together as

$$-q\int_0^\infty d\mathrm{r}\,\mathrm{r}^{J+1}\rho_o(i,f,\mathrm{r})\left[\frac{d}{d(q\mathrm{r})} + \frac{J+1}{q\mathrm{r}}\right] j_J(q\mathrm{r}) \qquad ...(17)$$

$$\left[\frac{d}{d(q\mathrm{r})} + \frac{J+1}{q\mathrm{r}}\right] j_J(q\mathrm{r}) = j_{J-1}(q\mathrm{r}) \qquad ...(18)$$

therefore

$$\int_0^\infty d\mathrm{r}\ \mathrm{r}^{J+1} j_J(q\mathrm{r})\frac{d\rho_o(i,f,\mathrm{r})}{d\mathrm{r}} = -q\int_0^\infty d\mathrm{r}\,\mathrm{r}^{J+1} j_{J-1}\rho_o(i,f,\mathrm{r}) \qquad ...(19)$$

Hence, the form factor of equation 15 takes the form

$$F^L_J(q) = \left(\frac{4\pi}{2J_i+1}\right)^{1/2}\frac{1}{Z}\left\{\int_0^\infty \mathrm{r}^2 j_J(q\mathrm{r})\overset{ms}{\rho}_{Jt_z}d\mathrm{r} - Nq\int_0^\infty d\mathrm{r}\,\mathrm{r}^{J+1}\rho_o\, j_{J-1}(q\mathrm{r})\right\} \times F_{cm}(q)\,F_{fs}(q) \qquad ...(20)$$

The proportionality constant N can be determined from the form factor evaluated at q=k, i.e. substituting q=k in equation 20, we obtain

$$N = \frac{\int_0^\infty d\mathrm{r}\,\mathrm{r}^2 j_J(k\mathrm{r})\,\rho^{ms}_{Jt_Z}(i,f,\mathrm{r}) - F^L_J(k)\,Z\sqrt{\frac{2J_i+1}{4\pi}}}{k\int_0^\infty d\mathrm{r}\,\mathrm{r}^{J+1}\rho_o(i,f,\mathrm{r})\,j_{J-1}(k\mathrm{r})} \qquad ...(21)$$

The reduced transition probability *B(CJ)* is written in terms of the form factor in the limit $q = k$ (photon point) as (Brussard & Glaudemans, 1977)

$$B(CJ) = \frac{[(2J+1)!!]^2\,Z^2\,e^2}{4\pi\,k^{2J}}\left|F^L_J(k)\right|^2 \qquad ...(22)$$

In equation 22, the form factor at the photon point $q = k$ is related to the transition strength $B(CJ)$. Thus using equation 22 in equation 21 gives

$$N = \frac{\int_0^\infty dr\, r^2 j_J(kr)\rho^{ms}_{Jt_z}(i,f,r) - \sqrt{\frac{(2J_i+1)B(CJ)}{[(2J+1)!!]^2}}\,k^J}{k\int_0^\infty dr\, r^{J+1}\rho_o(i,f,r)\, j_{J-1}(kr)} \quad ...(23)$$

where (Radhi & Aouda, 1997)

$$j_j(kr) = \frac{(kr)^J}{(2J+1)!!} \text{ and } J_{J-1}(kr) = \frac{(kr)^{J-1}}{(2J-1)!} \quad ...(24)$$

Introducing equation 24 into equation 23, we obtain

$$N = \frac{\int_0 dr\, r^{J+2}\rho^{ms}_{Jt_z}(i,f,r) - \sqrt{(2J_i+1)B(CJ)}}{(2J+1)\int_0^\infty dr\, r^{2J}\rho_o(i,f,r)} \quad ...(25)$$

The proportionality constant N can be determined by adjusting the reduced transition probability $B(CJ)$ using equation 25 with the experimental value of $B(CJ)$.

RESULTS AND DISCUSSION

The inelastic longitudinal electron scattering form factors are calculated using the expression for the transition charge density. The model space transition density is obtained using equation 9, where the OBDM elements are taken from the interaction matrix elements of Cohen-Kurath (CK) (Lee & Kurath, 1980) and Wildenthal (W) (Brown *et al.*, 1983) for 1p-shell and 2s-1d shell nuclei, respectively. For considering the collective modes of the nuclei, the core polarization transition density of equation 12 is evaluated by adopting the Tassie model (Flaiyh, 2010) together with the ground state two-body charge density distributions of equation 13.

In Figures 1- 4, the calculated results for inelastic longitudinal form factors of all nuclei under the study are plotted versus the momentum transfer q and compared with those of experimental results for the transitions $\left(J_i^\pi T_i \rightarrow J_f^\pi T_f\right)$. It is important to point out that all transitions considered in the present work are of an isoscalar character. In addition, the parity of these transitions does not change.

Closed shell nuclei

Let us first explore the calculated results for some light

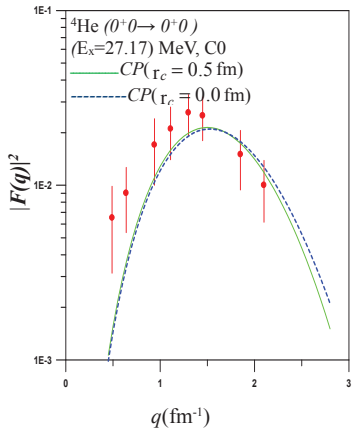

a. Inelastic longitudinal C0 form factors for ^{4}He nucleus. The solid circle symbols (Abgralh Y. & Caurier E., 1975).

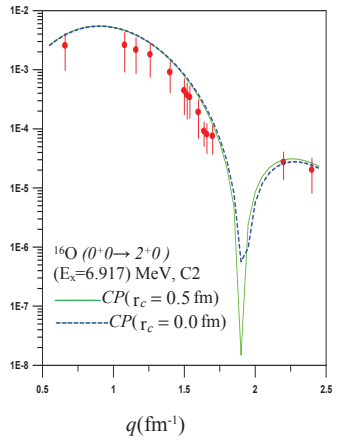

b. Inelastic longitudinal C2 form factors for ^{16}O nucleus. The solid circle symbols (Norum B.E. *et al.*, 1982).

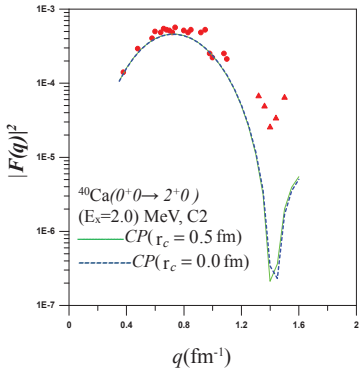

c. Inelastic longitudinal C2 form factors for ^{40}Ca nucleus. The solid circle symbols (Starodubsky V.E., 1974) and triangle symbols (Abgralh Y. & Caurier E., 1975).

Figure 1: Inelastic longitudinal form factors for a. ^{4}He, b. ^{16}O and c. ^{40}Ca nuclei.

closed shell ^{4}He, ^{16}O, and ^{40}Ca nuclei. These nuclei are cores of closed shell only, i.e. there are no valence (active) particles moving outside these cores. Therefore, these nuclei have no model space contribution, i.e. the longitudinal form factors of these nuclei comes totally from the core polarization only. Figure 1-a shows the inelastic longitudinal C0 form factors for the transition $0_1^+ 0 \rightarrow 0_2^+ 0$ in ^{4}He nucleus. In this transition, the electron excites the nucleus from the ground state $0_1^+ 0$ to the excited state $0_2^+ 0$ with an excitation energy of E_x = 27.17 MeV. The experimental reduced transition probability B(C0) is equal to 2.02 ± 0.32 e^2.fm^2 (Abgralh & Caurier, 1975). The solid and dashed curves are the calculated core polarization form factors with and without the inclusion of the effect of the short range correlation (SRC) while the dotted symbols are those of experimental data taken from Abgralh and Caurier (1975). It is obvious from this figure that the calculated C0 form factors (the dashed and solid curves) predict the data clearly throughout the whole range of momentum transfer q. The inelastic longitudinal C2 form factors for the transition $0_1^+ 0 \rightarrow 2_1^+ 0$ in ^{16}O nucleus is presented in Figure 1-b. Here, the nucleus is excited from the ground state $0_1^+ 0$ to the state $2_1^+ 0$ with an excitation energy of E_x = 6.917 MeV. The experimental reduced transition probability B(C2) is equal to 40 ± 10.8 e^2. fm^4 (Gulkarov & Vakil, 1986). The C2 form factors of ^{16}O nucleus with and without the effect of SRC's (the solid and dashed curves, respectively) are in satisfactory agreement with the experimental data (Norum *et al.*, 1982). It is clear that the magnitude of the C2 form factor along the first and second maximum are very well reproduced. Furthermore, the measured diffraction minimum is reproduced at the correct momentum transfer. In Figure 1-c the inelastic longitudinal C2 form factors for the transition $0_1^+ 0 \rightarrow 2_1^+ 0$ in ^{40}Ca nucleus are presented. In this transition the nucleus is excited by the electron from the ground state $0_1^+ 0$ to the excited state $2_1^+ 0$ with an excitation energy of E_x = 2.0 MeV. The experimental reduced transition probability B(C2) is equal to 84 ± 3.0 e^2.fm^4 (Starodubsky, 1974). The solid and dashed curves are the C2 form factors of ^{40}Ca nucleus with and without the effect of SRCs respectively, whereas the dotted and triangle symbols are those of measured data of Starodubsky (1974) and Abgralh and Caurier (1975), respectively. The available data of this transition are restricted for a small region of momentum transfer (q < 1.4 fm^{-1}). In the first maximum, a best coincidence for the form factors is obtained between the calculation (the dashed and solid curves) and the experimental data, i.e. the calculated form factors are in good agreement with the experimental data up to momentum transfer region of $q \leq 1$ fm^{-1}. While for $1 \leq q \leq$ 1.4 fm^{-1} the data is underestimated by the calculated results. However, the behaviour of the calculated C2 form factors agrees

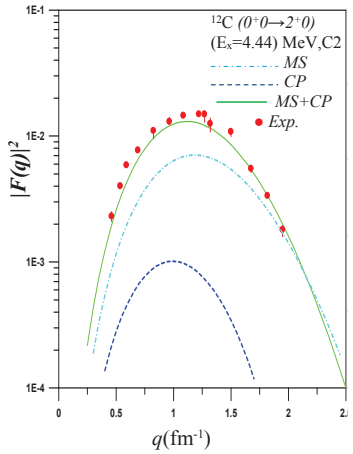

a. Inelastic longitudinal C2 form factors for ^{12}C nucleus. The solid circle symbols (Flanz J.B. *et al*., 1978).

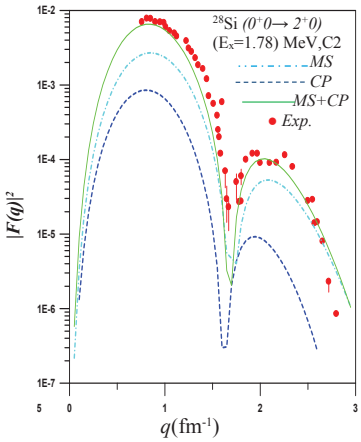

b. Inelastic longitudinal C2 form factors for ^{28}Si nucleus. The solid circle symbols (Whitner K. *et al*., 1980).

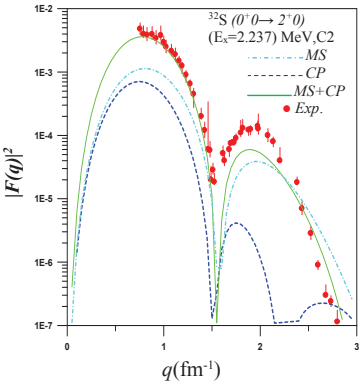

c. Inelastic longitudinal C2 form factors for ^{32}S nucleus. The solid circle symbols (Li G.C. *et al*., 1974).

Figure 2: Inelastic longitudinal C2 form factors for a. ^{12}C, b. ^{28}Si and c. ^{32}S nuclei.

Table 1: The values of the OBDM elements for the longitudinal C2 form factors of the isoscalar transition (2^+0) at E_x = 4.44 MeV for ^{12}C (Lee & Kurath, 1980).

$2j_i$	$2j_f$	OBDM ($\Delta T = 0$)
3	3	0.0000000
3	2	0.7591841
2	3	- 0.5011840
2	2	- 0.3097547

Table 2: The values of the OBDM elements for the longitudinal C2 form factors of the isoscalar transition (2^+0) at E_x = 1.78 MeV for ^{28}Si (Brown *et al.*, 1983).

$2j_i$	$2j_f$	OBDM ($\Delta T = 0$)
5	5	- 0.2986
5	1	- 0.4066
5	3	- 0.3038
1	5	- 0.5949
1	3	- 0.0862
3	5	0.3835
3	1	0.1532
3	3	- 0.1714

Table 3: The values of the OBDM elements for the longitudinal C2 form factors of the isoscalar transition (2^+0) at E_x = 2.237 MeV for ^{32}S (Brown *et al.*, 1983).

$2j_i$	$2j_f$	OBDM ($\Delta T = 0$)
5	5	- 0.0701
5	1	- 0.1542
5	3	- 0.1105
1	5	- 0.2155
1	3	- 0.3730
3	5	0.1178
3	1	0.6000
3	3	- 0.2492

quite well with the experimental data. In addition, the calculated results for the C2 form factors reproduce the diffraction minimum at the correct momentum transfer.

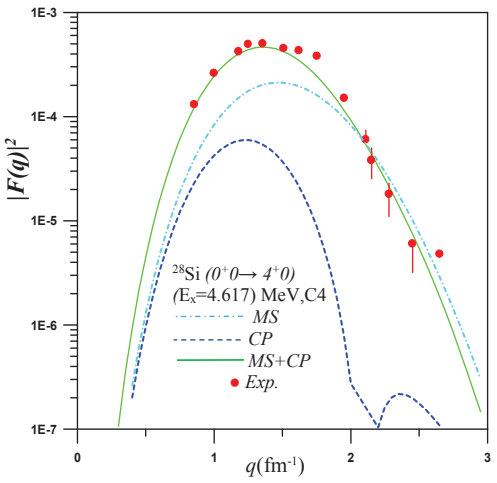

Figure 3: Inelastic longitudinal C4 form factors for ^{28}Si nucleus. The solid circle symbols (Whitner K. *et al*., 1980).

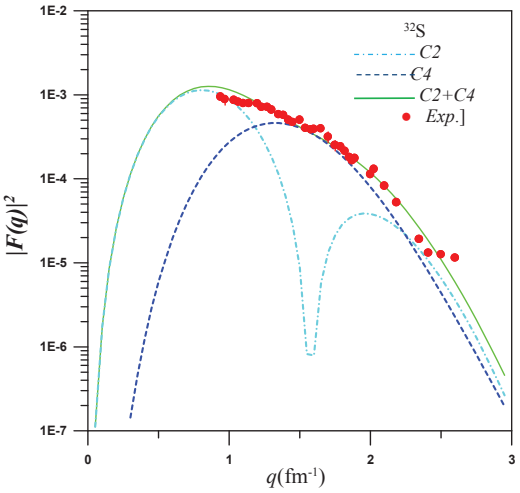

Figure 4: Experimental and theoretical form factors for the 4.282 MeV 22+ + 4.46 MeV 41+ doublets in ^{32}S. The solid circle symbols (Wildenthal B.H. *et al*., 1985).

Table 4: The values of the OBDM elements for the longitudinal C4 form factors of the isoscalar transition (4^+0) at E_x = 4.617 MeV for ^{28}Si (Brown *et al.*, 1983).

$2j_i$	$2j_f$	*OBDM* ($\Delta T = 0$)
5	5	- 0.0032
5	3	- 0.2413
3	5	0.4981

Open shell nuclei

The inelastic longitudinal C2 form factors of ^{12}C, ^{28}Si and ^{32}S open shell nuclei are presented in Figure2-a, b and c, respectively. Here, the calculated longitudinal C2 form factors are plotted as a function of the momentum transfer (q) for the transitions, $\left(J_i^\pi T_i \rightarrow J_f^\pi T_f\right), 0^+0 \rightarrow 2_1^+0$ (E_x = 4.44) MeV, B(C2) = 38.81 ± 2.15 e^2.fm^4 (Yen *et al.*, 1974) in ^{12}C , $0^+0 \rightarrow 2_1^+0$ (E_x = 1.78) MeV, B(C2) = 327.24 ± 9.47 e^2.fm^4 (Brown *et al.*, 1983) in ^{28}Si and $0^+0 \rightarrow 2_1^+0$ (E_x = 2.237) MeV, B(C2) = 300.33 ± 11.9 e^2.fm^4 (Brown *et al.*, 1983) in ^{32}S. In this figure; the dash- dotted curves represent the contribution of the model space where the configuration mixing is taken into account; the dashed curves represent the core polarization contribution where the effect of SRCs is considered; the solid curves represent the total contribution, which is obtained by taking the model space together with the core polarization effects into consideration and the dotted symbols represent the experimental data of ^{12}C (Flanz *et al.*, 1978), ^{28}Si (Whitner *et al.*, 1980) and ^{32}S (Li *et al*., 1974). The OBDM elements for the above transitions are given in Tables 1, 2 and 3 for ^{12}C, ^{28}Si and ^{32}S nuclei, respectively. This figure shows that the contribution of the model space cannot reproduce the experimental data since it underestimates the data for all values of momentum transfer. Considering the effect of core polarization together with the model space (the solid curves) leads to enhancement of the longitudinal C2 form factors and consequently makes the calculated results satisfactorily describe the experimental data for all values of momentum transfer q. The inelastic longitudinal C4 form factors for ^{28}Si are displayed in Figure 3. Here, the electron excites the ^{28}Si nucleus from the ground state ($J_i^\pi T_i = 0_1^+0$) to the excited state ($J_f^\pi T_f = 4_1^+0$) with an excitation energy of 4.617 MeV. The experimental reduced transition probability B(C4) is equal to $27.5 \pm 5.0 \times 10^3$ e^2.fm^8 (Brown *et al.*, 1983).The values of the one-body density matrix elements (OBDM) for this transition are illustrated in Table 4. In this figure, the contribution of the model space is represented by the dash-dotted curve, the core polarization contribution with the effect of the SRC's is represented by the dashed curve and the total contribution is represented by the solid curve and is obtained by taking the model space together with the core polarization effects into consideration. This figure shows that the model space is not able to give a satisfactory description with the experimental data for the region of momentum transfer $q < 2$ fm^{-1} but once the core polarization effect is added to the model space, the results obtained for the longitudinal C4 form factors show good agreement with the experimental data throughout the whole range of momentum transfer q. Figure 4 presents the form factors for the combination of the first ($J_f^\pi T_f = 4_1^+0$) state [with excitation energy 4.46 MeV and B(C4) = 49.9 e^2.fm^8 (Wildenthal *et al*., 1985)] and the second ($J_f^\pi T_f = 2_2^+0$) state [with excitation energy 4.482 MeV and B(C2) = 6.65 ± 0.48 e^2.fm^4 (Brown *et al.*, 1983)] of ^{32}S nucleus. The one-body density matrix elements for these transitions are shown in Tables 5 and 6. Many attempts were made to explain the C4 transition in the upper half of the 2s-1d shell nuclei for the mass region ($30 \leq A \leq 40$). In this region, there is no available data for the C4 electron scattering that can be used in the analysis. The most logical candidate for improving this situation would seem to be the ^{32}S nucleus where extensive C2 results are available. The main difficulty that prevents the calculations from being improved with the ^{32}S nucleus is concerned with the closeness of the first 4_1^+0 and the second 2_2^+0 states in which their experimental energy separation is quite small, which prevents the experiments of electron scattering of resolving them. However, the calculated form factors of ^{32}S doublet is presented in Figure 4. The dash-dotted curve represents the total C2 form factors, which includes both contributions of the model space and core polarization effect; the dashed curve represents the total C4 form factors with both contributions; the solid

Table 5: The values of the OBDM elements for the longitudinal C2 form factors of the isoscalar transition (2_2^+0) at E_x = 4.282 MeV for ^{32}S (Brown *et al.*, 1983).

$2j_i$	$2j_f$	OBDM (ΔT = 0)
5	5	0.0906
5	1	0.1547
5	3	0.1557
1	5	0.2620
1	3	0.0456
3	5	- 0.4069
3	1	- 0.0516
3	3	- 0.1443

Table 6: The values of the OBDM elements for the longitudinal C4 form factors of the isoscalar transition (4^+0) at E_x = 4.46 MeV for ^{32}S (Brown *et al.*, 1983).

$2j_i$	$2j_f$	OBDM (ΔT = 0)
5	5	- 0.0819
5	3	- 0.2690
3	5	0.5603

curve represents the sum of C2 and C4 contributions and the dotted symbols represent the experimental form factors taken from Wildenthal *et al*. (1985). Beyond 1.4 fm^{-1} ($q > 1.4$ fm^{-1}) the form factor is predicted to be nearly totally from C4 excitation (Figure 4). In general, the comparison between the experimental data and the combined 2_2^+0 and 4_1^+0 calculated form factors is in excellent agreement since the solid curve shows a nice consistency with the available data.

CONCLUSION

The effect of the inclusion of the two-body short range correlations is small in the calculations of the inelastic longitudinal form factors of closed shell nuclei and it even becomes gradually smaller with increase of the mass number A of closed shell nuclei. The core polarization effects, which represent the collective modes are essential in obtaining a remarkable agreement between the calculated inelastic longitudinal *F(q)*'s and those of experimental data for all considered nuclei.

Acknowledgement

We thank the Islamic Development Bank (IDB) for supporting this work (grant No. 36/11201905/35/IRQ/D31). The Department of Physics, Faculty of Science, University of Malaya; the Department of Physics, College of Science, University of Karbala; and the Department of Physics, College of Science, University of Baghdad are also acknowledged for the support.

REFERENCES

1. Abgralh Y. & Caurier E. (1975). On the monopole and quadrupole isoscalar giant resonances in ^{4}He, ^{16}O, ^{20}Ne and ^{40}Ca. *Physics Letters* **56B**: 229 − 231.
2. Brown B.A., Wildenthal B.H., Williamson C.F., Rad F.N., Kowalski S., Hall Crannell & O'Brien J.T. (1985). Shell-model analysis of high-resolution data for elastic and inelastic electron scattering on ^{19}F. *Physical Reviews C* **32**: 1127 − 1156. DOI: http://dx.doi.org/10.1103/PhysRevC.32.1127
3. Brown B .A., Radhi R. & Wildenthal B.H. (1983). Electric quadrupole and hexadecupole nuclear excitations from the perspectives of electron scattering and modern shell-model theory. *Physics Reports* **101**: 313 − 358. DOI: http://dx.doi.org/10.1016/0370-1573(83)90001-7
4. Brussard P.J. & Glaudemans P.M. (1977). *Shell-Model Applications in Nuclear Spectroscopy*, pp.200. Amsterdam, North Holland.
5. Donnelly T.W. & Sick I. (1984). Elastic magnetic electron scattering from nuclei. *Reviews of Modern Physics* **56**: 461 − 566. DOI: http://dx.doi.org/10.1103/RevModPhys.56.461
6. Flaiyh G.N. (2010). Transition charge distributions in nuclear collective modes. *Journal of the Al-Nahrain University* **13**: 58 − 64.
7. Flanz J.B., Hicks R.S., Lindgren R.A., Peterson G.A., Hotta A., Parker B. & York R.C (1978). Convection Currents and Spin Magnetization in E2 Transitions of ^{12}C. *Physical Review Letters*. **41**: 1642 − 1645. DOI: http://dx.doi.org/10.1103/PhysRevLett.41.1642
8. Gulkarov I. S. & Vakil R. Kh. (1986). Form factors and transition densities of charge of ^{16}O and ^{18}O Nuclei. *Yadernaya fizika* **43**: 809 − 314.
9. Hotta A., Dubach J., Hicks R.S., Huffmann R.L., Parker B., Peterson G.A., Ryan P. J., Singhal R.P. & Halderson D. (1988). Electroexcitation of ^{4}He in the near continuum. *Physical Reviews C* **38**: 1547 − 1551. DOI: http://dx.doi.org/10.1103/PhysRevC.38.1547
10. Lee T.-S. & Kurath D. (1980). Inelastic pion scattering for 1p-shell targets. *Physical Reviews* C **21**: 293 − 305. DOI: http://dx.doi.org/10.1103/PhysRevC.21.293
11. Li G. C., Yearian M. R. & Sick I. (1974). High-momentum-transfer electron scattering from ^{24}Mg. *Physical Reviews C* **9**: 1861 − 1877. DOI: http://dx.doi.org/10.1103/PhysRevC.9.1861
12. Millener D. J., Sober D.I., Crannell H., O'Brien J.T., Fagg L.W. & Lapikás L. (1989). Inelastic electron scattering from ^{13}C. *Physical Reviews* **39**: 14 − 46.
13. Miska H., Gräf H.D., Richter A., Schneider R., Schüll D., Spamer E., Theissen H., Titze O. & Walcher Th. (1975). High resolution inelastic electron scattering and radiation widths of levels in ^{16}O. *Physics Letters* **58B**: 155 − 158.
14. Norum B.E., Hynes M.V., Miska H., Bertozzi W., Kelly J Kowalski S., Rad F.N., C. Sargent P., Sasanuma T., Turchinetz W. & Berman B.L. (1982). Inelastic electron scattering from ^{18}O**.** *Physical Reviews C* **25**: 1778 − 1800. DOI: http://dx.doi.org/10.1103/PhysRevC.25.1778
15. O'Connell J.S., Hayward E., Lightbody J.W., Jr., Maruyama X.K., Bosted P., Blomqvist K.I., Franklin G., Adler J.-O., Hansen K., & Schroder B. (1983). Total nuclear inelastic electron scattering cross sections compared to sum rule calculations. *Physical Reviews C* **27**: 2492 − 2499. DOI: http://dx.doi.org/10.1103/PhysRevC.27.2492
16. Radhi R.A. & Aouda A. (1997). Inelastic electron scattering form factors for the one proton-hole state in the p-shell and sd-shell nuclei. *Proceedings of the first Scientific Conference* **1**: 297 − 305.
17. Radhi R.A. & Boucheback A. (2003). Microscopic calculations of C2 and C4 form factors in *sd*-shell nuclei. *Nuclear Physics A* **716**: 87 − 99. DOI: http://dx.doi.org/10.1016/S0375-9474(02)01335-0
18. Radhi R.A. (2003). Core polarization effects on C4 form factors of sd-shell nuclei. *European Physical Journal A* **16**: 381 − 385. DOI: http://dx.doi.org/10.1140/epja/i2002-10065-1
19. Radhi R.A., Al-Rahmani A., Hamoudi A.K. & Salman E.A. (2002). Transition charge distribution in nuclear collective modes. *Iraqi Journal of Science C* **43**: 27 − 32.

20. Sharrad F. I. (2007). The effect of two body short range correlation functions on the charged density distributions and form factors of some light nuclei. *Ph.D. thesis*, University of Baghdad, Baghdad, Iraq.
21. Starodubsky V.E. (1974). The excitation of collective nuclear states by high energy particles. *Nuclear Physics A* **219**: 525 − 542.
DOI: http://dx.doi.org/10.1016/0375-9474(74)90115-8
22. Whitner K., Williamson C.F., Norum B. E. & Kowalski S. (1980). Inelastic electron scattering from ^{29}Si. *Physical Reviews C* **22**: 374 − 383.
DOI: http://dx.doi.org/10.1103/PhysRevC.22.374
23. Wildenthal B.H., Brown B A. & Sick I. (1985). Electric hexadecupole transition strength in ^{32}S and shell-model predictions for E4 systematics in the sd shell. *Physical Reviews C* **32**: 2185 − 2188.
DOI: http://dx.doi.org/10.1103/PhysRevC.32.2185
24. Yamaguchi A., Terasawa T., Nakahara K. & Torizuka Y. (1971). Excitation of the Giant Resonance in ^{12}C by Inelastic Electron Scattering. *Physical Reviews C* **3**: 1750 − 1769.
DOI: http://dx.doi.org/10.1103/PhysRevC.3.1750
25. Yen R., Cardman L., SKalinsky D., Legg J.R. & Bockelman C.K. (1974). Determination of nuclear parameters by inelastic electron scattering at low-momentum transfer. *Nuclear Physics A* **235**: 135 − 153.
DOI: http://dx.doi.org/10.1016/0375-9474(74)90182-1